MiR
2012

AGI
Associazione
Geotecnica
Italiana

Nuovi metodi di indagine monitoraggio e modellazione degli ammassi rocciosi

www.symposium.it/mir2012

TORINO
21-22 novembre 2012

POLITECNICO DI TORINO
1859 1906

Aula Magna
del Politecnico di Torino
Corso Duca degli Abruzzi 24

COMITATO ORGANIZZATORE

Giovanni Barla *(coordinatore)*
Marco Barla, Anna Maria Ferrero, Tatiana Rotonda

PROGRAMMA SCIENTIFICO

Nuovi metodi di indagine, monitoraggio e modellazione degli ammassi rocciosi

Mercoledì 21 Novembre 2012

8.00 Registrazione partecipanti

9.00 Introduzione

Nuovi metodi di indagine

9.15 Rock engineering, uncertainty and Eurocode 7: implications for rock mass characterization. *J. Harrison (University of Toronto, Canada)*

10.00 Innovazione nella sperimentazione in laboratorio e in sito. *G. Barla, M. Barla (Politecnico di Torino)*

10.30 *Coffee break*

11.00 Valutazione della resistenza al taglio delle discontinuità con l'ausilio del laser scanner. *N. Nocilla, R. Sciortino, M. Zimbardo (Università degli Studi di Palermo)*

11.30 Innovazione nei rilievi geostrutturali. *A. M. Ferrero (Università degli Studi di Parma), R. Migliazza (Università degli Studi di Milano), G. Umili (Università degli Studi di Parma)*

12.00 Discussione

12.30 *Pausa*

Nuovi metodi di monitoraggio

14.00 Innovazione nelle tecniche di monitoraggio tradizionali. *G. Barla (Politecnico di Torino), A. Morino (GD Test, Torino)*

14.30 Tecniche InSAR avanzate per la valutazione del rischio di frana, dei tassi di subsidenza e per il monitoraggio delle infrastrutture in fase di costruzione e di esercizio. *A. Tamburini, S. Del Conte, A. Ferretti, C. Giannico (T.R.E., Milano)*

15.00 Applicazione di nuove tecnologie di indagine e monitoraggio per fenomeni di instabilità in ammassi rocciosi. *N. Casagli, G. Gigli (Università degli Studi di Firenze)*

15.30 Discussione

16.00 *Coffee break*

Nuovi metodi di modellazione

16.30 From analytical closed form solutions to conventional and advanced numerical modelling in rock engineering applications. *L. R. Alejano (University of Vigo, Spain)*

17.15 Analisi agli elementi distinti per gli ammassi rocciosi. *F. Calvetti (Politecnico di Milano)*

Giovedì 22 Novembre 2012

Nuovi metodi di modellazione (continua)

8.30 La Meccanica della Frattura per lo studio della rottura in ammassi rocciosi fratturati a bassa persistenza. *M. Castelli, C. Scavia (Politecnico di Torino)*

9.15 Numerical simulations of scale effects for naturally fractured rock masses using a an hybrid FDEM approach and implications for rock mass strength characterisation. *D. Elmo (University of British Columbia, Vancouver, Canada)*

10.00 Discussione

10.30 *Coffee break*

Applicazioni

11.00 Integrazione tra monitoraggio e modellazione delle grandi frane in roccia nell'ottica dell'allertamento rapido. *F. Antolini, M. Barla (Politecnico di Torino)*

11.30 Indagini e modellazioni per lo studio di una frana in roccia in rapida evoluzione: il caso della frana di Mt del La Saxe. *G. B. Crosta (Università degli Studi di Milano - Bicocca)*

12.15 Some remarks on current rock engineering design practies in tunneling. *W. Schubert (University of Graz, Austria)*

13.00 *Pausa*

14.30 Modelling the failure modes of dam's rock foundations. *J. V. Lemos (Laboratório Nacional de Engenharia Civil LNEC, Lisbona)*

15.15 ***Tavola rotonda***
Quale beneficio dalle innovazioni per la sicurezza dei cantieri e la gestione dei problemi di protezione civile.

17.00 Chiusura dei lavori

Modalità di iscrizione

Per iscriversi alle Conferenze occorre compilare il modulo di iscrizione e trasmetterlo alla Segreteria Organizzativa via fax (011 9224992).

- Oltre alle iscrizioni individuali è prevista la possibilità effettuare iscrizioni collettive per gruppi formati da un massimo di tre persone appartenenti allo stesso Ente.

- L'iscrizione individuale include una copia degli Atti contenenti le memorie che sarà consegnata in sede di Conferenza. L'iscrizione collettiva darà diritto a due copie degli Atti.

- Non saranno registrate le richieste che perverranno prive del giustificativo di pagamento della quota d'iscrizione (bonifico bancario effettuato o autorizzazione all'addebito su carta di credito). Per l'applicazione della tipologia di quota farà fede la data del versamento.

Non sono previsti rimborsi sulle quote già versate.

- Sono previste quote individuali e collettive "early registration" a tariffa agevolata per gli iscritti del MIR 2010 e per i soci AGI.

Il modulo d'iscrizione è scaricabile sul sito: *www.symposium.it/mir2012*

Quote di iscrizione

Iscrizioni individuali "early registration", entro 28/9: € 330,00 + IVA 21%
Iscrizioni individuali "early registration", entro 28/9, iscritti MIR 2010 e soci AGI: € 300,00 + IVA 21%
Iscrizioni individuali "late registration": € 400,00 + IVA 21%

Iscrizioni collettive "early registration", entro 28/9: € 660,00 + IVA 21%
Iscrizioni collettive "early registration", entro 28/9, iscritti MIR 2010 e soci AGI: € 600,00 + IVA 21%

Iscrizioni collettive "late registration": € 800,00 + IVA 21%

Iscrizioni studenti (richiesta fotocopia del documento comprovante la qualifica): € 150,00 + IVA 21%

Segreteria Organizzativa

SYMPOSIUM

Via Gozzano 14 - 10073 Ciriè, Torino
Infoline 011 921.14.67 - Fax 011 922.49.92
info@symposium.it · www.symposium.it

Capitolo XXX

Studio di una frana in roccia in rapida evoluzione: il caso della frana di Mt. de la Saxe

Comprehensive understanding of a rapid moving rockslide: the Mt de la Saxe landslide

Crosta, G.B., Castellanza R., Frattini, P.

Dip. Scienze Geologiche e Geotecnologie, Univ. Studi di Milano Bicocca, Milano, ITALY

Broccolato M., Bertolo, D.,

Regione Autonoma Valle D'Aosta

Cancelli P.,

Studio Cancelli Associato, Milano, ITALY

Tamburini A,

Imageo, Torino, Italy

1 Introduction

Rockslides which can undergo a rapid evolution represent a major risk in alpine areas, requiring a careful study and monitoring, both for civil protection actions and to plan slope stabilization approaches. These types of landslide can occur high on the valley flanks increasing the risk over large areas of the valley bottom and can rapidly evolve in a relatively short time due to the progressive failure of the rock mass or to an external agent which can trigger instability.

At the same time, such phenomena can reach very large volumes. This makes their stabilization technically difficult, or prohibitive in terms of sustainable costs. As a consequence, the characteristics of such phenomena require the adoption of a complex multi-step approach which can be difficult to apply in emergency conditions, when the landslide is in an advanced evolutionary phase, with large displacements already occurred and a strong sensitivity to external actions.

We present here the case study of the Mont de La Saxe rockslide in the Courmayeur municipality (Aosta Valley, Italy) as a complex example of investigation because of the environmental and local risk constrains. This is an active rock slide characterized by a high risk because of its position above the Entrèves village, and its proximity to the Mont Blanc highway and tunnel, to the Mont Blanc cableway and to the access of some important tributary valleys. As a consequence, the possible impact on the area can be important both from the social and economic point of view and a

complete understanding of the process is desirable. In the following we will present the adopted approach subdivided in successive and iterative steps as schematized in Figure 1.
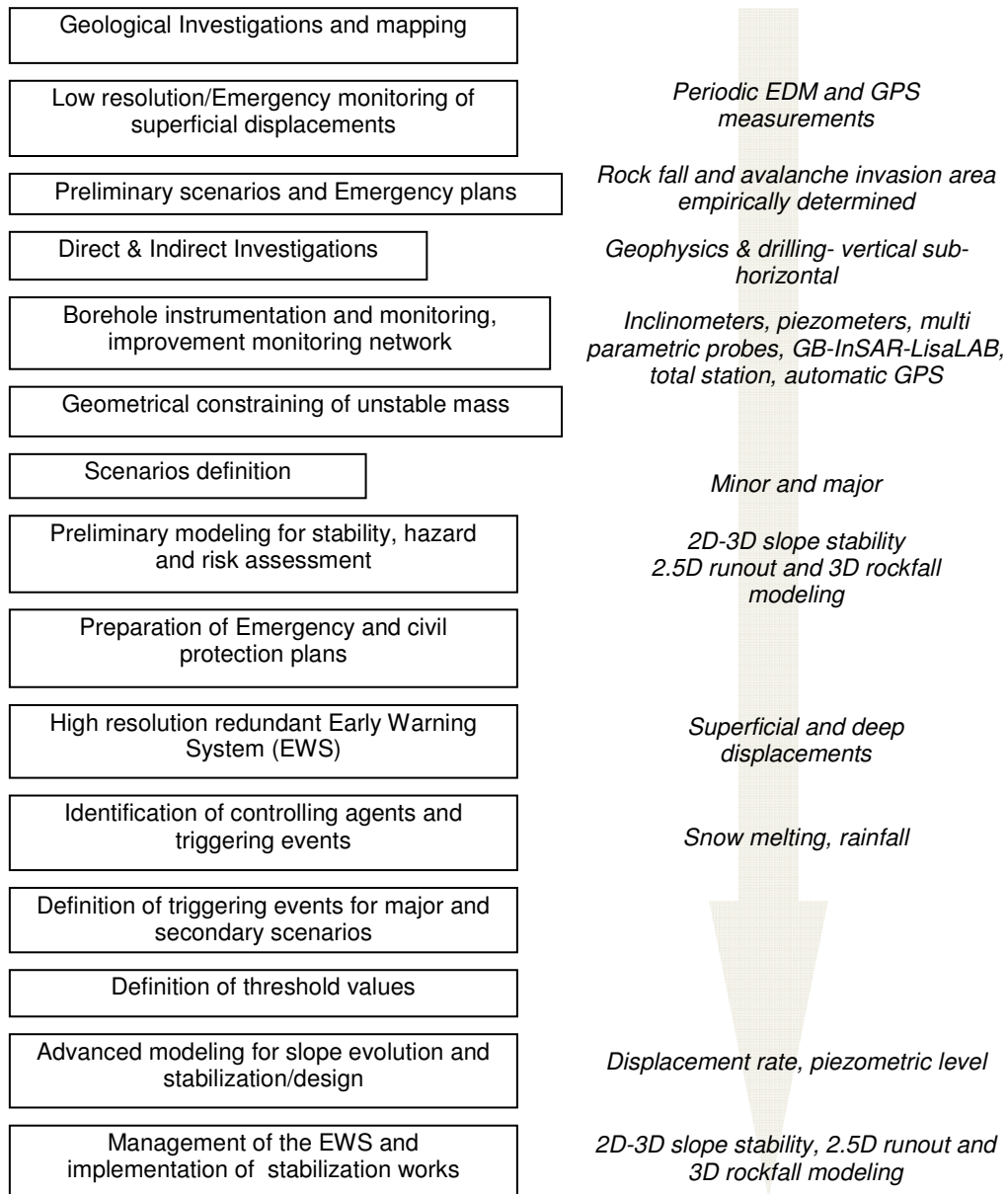
Geological Investigations and mapping	
Low resolution/Emergency monitoring of superficial displacements	*Periodic EDM and GPS measurements*
Preliminary scenarios and Emergency plans	*Rock fall and avalanche invasion area empirically determined*
Direct & Indirect Investigations	*Geophysics & drilling- vertical sub-horizontal*
Borehole instrumentation and monitoring, improvement monitoring network	*Inclinometers, piezometers, multi parametric probes, GB-InSAR-LisaLAB, total station, automatic GPS*
Geometrical constraining of unstable mass	
Scenarios definition	*Minor and major*
Preliminary modeling for stability, hazard and risk assessment	*2D-3D slope stability 2.5D runout and 3D rockfall modeling*
Preparation of Emergency and civil protection plans	
High resolution redundant Early Warning System (EWS)	*Superficial and deep displacements*
Identification of controlling agents and triggering events	*Snow melting, rainfall*
Definition of triggering events for major and secondary scenarios	
Definition of threshold values	
Advanced modeling for slope evolution and stabilization/design	*Displacement rate, piezometric level*
Management of the EWS and implementation of stabilization works	*2D-3D slope stability, 2.5D runout and 3D rockfall modeling*

Figure 1. Summary of the main activities performed for the Mt de la Saxe rock slide. Some of the actions (e.g. borehole drilling, monitoring, modeling) have been repeated at different stages to improve the level of knowledge or the hazard and risk assessment or as a function of occurring events.

2 Geological settings

The Mt de La Saxe rockslide is located at the outlet of the Ferret valley, at the immediate foot of the Mont Blanc massif. The landslide, affecting the Ultra Helvetic cover along the left hand flank of the valley, is placed just N of the Penninic frontal thrust which separates low grade from very/extremely low grade metamophic rocks. The Helvetic - Ultra Helvetic domain is formed by intensely deformed meta-sedimentary rocks (Jurassic limestone-marly limestone, black schist and calcschist) in tectonic contact with the Chetif - Mont de La Saxe meta-granites and meta-rhyolites. The predominant black schists dip at varying angle and sometimes are subvertical along the slope and are interested by subvertical faults. The apparent schistosity seems more related to the pre-existing stratification than to an axial plane foliation. This seems also confirmed by the evidence collected by means of the boreholes drilled within the slope.

A large sector of the left hand valley flank is affected by a deep seated gravitational slope deformation with clear scarps and counterscarps, trenches and double ridges which are conditioned by the geometry of the geological and structural elements which have been activated by the slope instability.In fact some subvertical dextral faults are recognized in the area and can be passively reactivated by the gravitational slope deformation.

At the same time these morpho-structures strongly control the superficial drainage pattern along the slope, imposing an evident SW trend parallel to the slope direction. The valley bottom close to the Ferret valley outlet is characterized by a relatively steep topographic gradient causing a large elevation difference between the tributary and the main valley bottom. Figure 1 shows that the position of the Mt de la Saxe rockslide is coincident with the extreme SW limit of the Ferret valley and affect the lower half of the slope.
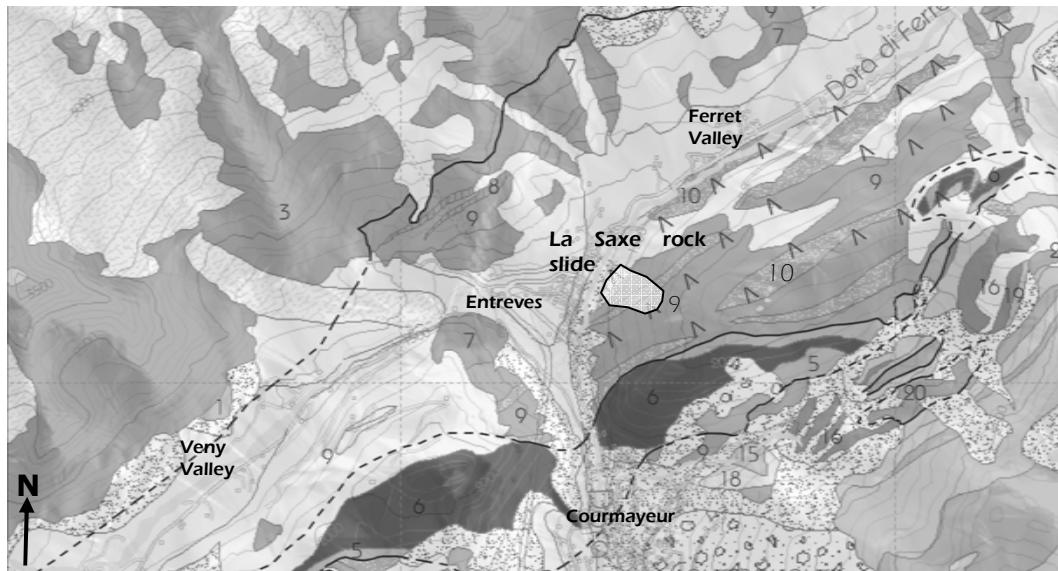

Figure 2. Geological map of the study area as from the Geological Map of the Aosta Valley (modified from De Giusti et al., 2005). 3) Mont Blanc granite; 5) Mt Chetif sedimentary cover: Liassic limestone; 6) meta-granites, meta-rhyolites with mylonitic overprint.7) limestones, and calcschists 8) limestones, 9) black clay schists and marly limestones 10) calcarénites. The upside down V represents the Deep Seated Gravitational Slope deformation along the left hand valley flank.

Figure 3. The left hand flank of the Ferret valley. Both the deep seated gravitational slope deformation and the Mont de La Saxe rock slide are visible, the latter located at the valley outlet (right hand side in the photo) just above the Entrèves village.

3 The Mont de La Saxe rockslide

The Mt de La Saxe rockslide is located in an area known as unstable since many years (Ratto et al, 2007), but very little information exists concerning its activity. The rock slide is located at the extreme SW tip of a deep seated gravitational slope deformation, which morpho-structures end against or are interrupted and disturbed by the rock slide (see Figure 3). This can be important at constraining both the landslide geometry and the presence of weakness zones with different physical mechanical properties with respect to the other slope sectors.

Since 2002 some of the authors of this contribution started worrying about the recent evolution of the phenomenon and for this reason displacement data (15 measurements) were collected up to 2009 for 8 optical targets by EDM (Electronic Distance Measurement) from two station points.

The rock slide (of about $8 *10^6$ m^3) develops between 1400 and 1870 m a.s.l., over an area of about 150.000 m^2, with a maximum length projected on the horizontal of about 550 m and a maximum width of about 420 m, and an average slope gradient of 37°. It can be subdivided in areas with different morphology and style of activity. The upper scarp is about 200 m wide and it is characterized by a steep rocky wall some tens of metres high locally controlled by foliation planes attitude.

The landslide head is quite irregular and characterized by a rapid evolution with opening and closing tension cracks and intensely broken rock mass. The downhill limit of the head is formed by a steep and irregular rocky wall, some of tens of meters high, below which a gentler slope continue almost up to the slope toe (almost 500 m wide) where an irregular and intensely broken rocky cliff develops. This is connected to the valley bottom by a well-developed scree slope, locally more active and interested by rock falls.

The landslide body can be subdivided in two sectors parallel to the slope, with a NE right hand sector (with width from 60 m to about 150 m moving downhill) more active and covered by abundant loose debris with only sparse vegetation. The SW or left hand sector is by far larger and well vegetated with less evidences of activity.

Multi-temporal analysis of aerial photos (1983, 1988, 1998) shows that in 1983 the upper slope

sector was intensely vegetated and no debris scree was present at the already existing small headscarp. The small debris flows and scree along the slope were also rare and started to be visible in 1988, along the lower slope sector. The rockslide activity increased since the late '90s and on the 1998 aerial photos the upper scarp activity became evident. Since then, activity increased and the occurrence of rockfalls at its toe (2008, 2012) started with blocks reaching the Dora di Ferret river course.
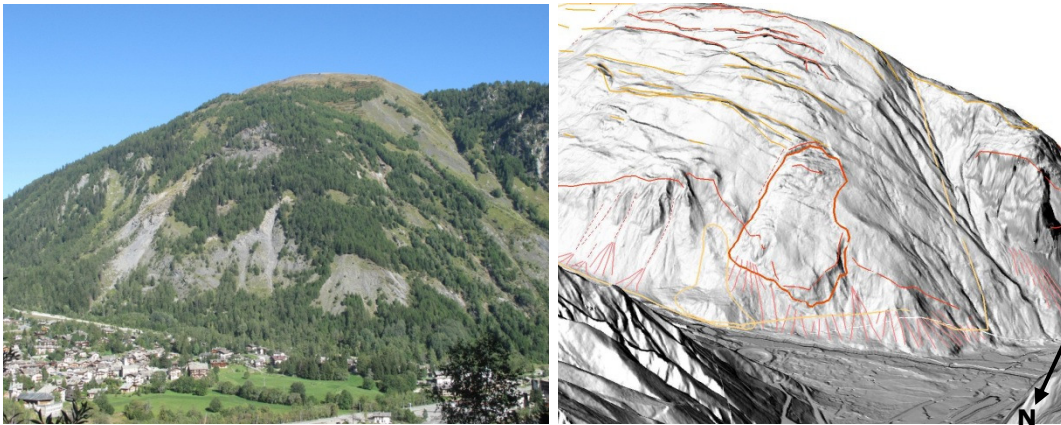

Figure 3. To the left a frontal view of the Mt de La Saxe rock slide with the scree slope material at the slide toe. To the right the shaded 1 m x 1 m LiDAR model which puts in evidence the orientation of the morpho-structures and their termination close to the rock slide crown area. A clear oblique feature develops from the left hand limit of the head scarp connecting to the major upslope counterscarps.

4 Investigations

The adopted investigation process included: geological and geomorphological mapping, geophysical seismic surveys, borehole drilling, in situ measurements. These investigations have been carried out in successive steps, to maximize the expected level of information that could be acquired.

4.1 Geophysical surveys

A total of 3.6 km seismic tomography surveys have been carried out along the slope (a longitudinal profile 1240 m long, and 4 transversal profiles ranging between 410 and 710 m in length) allowing the identification of three main layers characterized by different velocity of elastic waves ($Vp < 1.35$ km s^{-1}; $1.35 < Vp < 1.75$ km s^{-1} and $1.75 < Vp < 2.45$ km s^{-1}). These units extend to different depths ranging between 30 m and 50 m, 30 and 70 m, and 80 m, respectively. These units suggest the presence of a relaxed or fractured mass extending to depth up to 70-80 m below which some relatively sound rock is present. These sections do not exclude in any case the presence of possible deep-seated failure surfaces.

4.2 Borehole drilling

Borehole drilling along the slope has been performed through a series of campaigns. This was due to the environmental and logistic conditions. Due to the elevation of the slope the season to carry out drilling operations is relatively short (July to October) and the initial campaigns were conducted by airlifting the drilling equipment by helicopter. The last two campaigns (2011 and 2012) benefited

of a new small track directly reaching the landslide site. 14 boreholes have been drilled and 4 more are currently drilled along the slope. 11 inclined (22° to 29°) boreholes (110 to 180 m long) have been drilled and 2 more are currently under drilling. This relatively large number of boreholes have been drilled because of the complexity of the system, the need for a more complete and clear identification of water level within the landslide mass, and the monitoring requirements. These last have been influenced by the large displacement rate of the rock slide and the consequent damage and loss of efficiency of the drilled boreholes and instrumentation after one or two years.

RQD profiles along the boreholes clearly show the presence of a thick (30-90m) intensely fractured layer extending from the surface to a more compact bedrock. Brecciated levels were not frequent but in some cases intensely fractured material were found for thicknesses ranging between few centimeters and some meters. Foliation varies in inclination with respect to the borehole axis but it is frequently inclined between 20° and 40° with extremely rare subvertical orientation and seems more related to the pre-existing stratification. During the drilling of some inclined drains water pockets have been found which released water prevalently in a discontinuous way.

Finally, a more than 200 m deep borehole has been recently drilled within one of the upper trenches, about 70 m above the crown area. Here the rock resulted broken and extremely permeable for the entire length with only a very minor presence of water. This observation is interesting and will become important when considering the slope hydrogeological model.

4.3 Hydrogeological observations

Water or air losses were frequently observed during drilling through the upper 30 m to 90 m and in the upper layers, and no Lugeon test was feasible up to this depth. Water pockets have been found in two inclined boreholes, one of very short duration and another more continuous, with a relatively relevant discharge (about 1-2 l/s).

Springs have been mapped and monitored periodically along the slope. The most important springs are located a few hundred meters S of the head scarp more or less at the same elevation. One of them reaches discharges up to 10 - 40 l/s, during the snow melting season (May to end of June) and presents travertine like deposits with a water temperature similar to the average air temperature (2-4°C).

The area is subjected to snow precipitation during the winter (ave equivalent rainfall 810 mm ca., meteo-station of Mt de La Saxe at 2076 m a.s.l.) with a total average precipitation of about 1470 mm (at the rock slide crown area) and a real evapo-transpiration amounting to about 370 mm.

Snow melt controls the hydrogeology of the area, as witnessed by the significant response of the groundwater level within monitored piezometers to snow-melting events, with a time lag of about one week (Figure 7). The groundwater level does not show similar responses as a consequence of rainfall events (Figure 4 and 7).

The water infiltration seems strongly controlled in the area by the presence of the large morpho-structures and their infiltration characteristics. To this regard, it is worth to note that during a tracer test in one of these trenches, about 70 m above the main scarp, about 4000 liters of water transported in five tours (about 800 l each) by helicopter and discharged rapidly by a series of cloudburst fire bucket were rapidly absorbed by the soil. As said above, morpho-structures are parallel to the slope direction and control surface water runoff redirecting it towards the rock slide crown area, or facilitating its infiltration within the slope through the more permeable materials aligned with the trench direction. Because of this, the rockslide, and in particular the head scarp area, are probably fed by the water drained by the morpho-structures making this an important controlling factor of the rockslide reactivation. By drawing the hydrological superficial catchments conditioned by the morpho-structures, we obtain a 0.3 km^2 surface area for the catchment draining toward the upper spring area and a 0.28 km^2 basin draining directly within the rock slide scarp. Just to have a rough idea of the potential and considering the material properties, assuming an infiltration of 80% of the water from snow melting only, we obtain a mean water discharge of 6-10 l/s for the entire year at the small catchment outlets (or fed springs).

Tracer tests have been performed by introducing Na-fluorescein and Tynopal directly from the surface or from boreholes equipped with open case piezometers, and monitoring the arrival at

boreholes and springs by passive captors and continuous spectro-fluorometer measurements. These tests do not provide perfectly clear results with ideal restitution curves, but give the possibility to roughly estimate the transport velocity through the rock mass (Figure 4). At the same time, some tests allowed us to recognize that the systems are locally compartmentalized especially because of the effect of intensely fractured material present within the trenches and counterscarps (e.g. computed hydraulic conductivity of 10^{-3} m d^{-1} by point dilution testing). From observed first arrivals, the peak velocity is estimated as 10 to 20 m d^{-1}.

Within the slope the deep groundwater table is controlled at a larger scale by the position in correspondence of the extreme tip on the left hand valley flank where a large difference in elevation exists between the Ferret tributary valley and the main valley bottom. As a consequence, the deep groundwater table should sense the effect of both the secondary and main base levels, draining water from within the Ferret valley flank. Finally, after drilling operations, most of the boreholes showed water levels at or below the depth of the sound bedrock appearance.
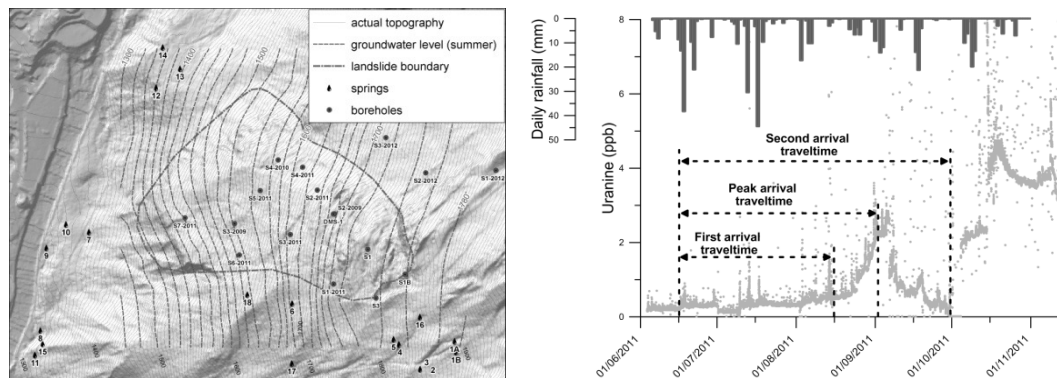
Figure 4. a) Piezometric water level during the summer period as from monitoring data, springs and borehole locations.. b) results of a Na-fluorescein tracer test

5 Monitoring

The level of potential risk associated to this rockslide makes mandatory the installation and use of a reliable and robust monitoring network to support the emergency and civil protection actions. At the same time the availability of monitoring data can be extremely useful to constrain the landslide geometry and its general behavior. In fact, monitoring can reveal information about the rock slide depth, the displacements at the surface or at depth, the sensitivity to external actions and the seasonality, as well the tendency to a final collapse or critical accelerations. Eventually, it makes feasible the definition of alert thresholds.

Because of the environmental conditions and the level of risk it has been decided to implement a redundant network (see Figure 5) able to give information under most critical conditions (e.g. rapid accelerations, adverse meteorological conditions, rapid movement of sectors of the rock slide, need for remote access to the data). As mentioned above, in the explorative phase, a simple EDM measuring system with periodic measurements have been used. After this initial phase, recognized the level of hazard, a complete monitoring system have been deployed including, in the order of installation:

- 9 GPS measuring points for periodic manual measurements;
- 1 GB-InSAR (LisaLab system, by Ellegi srl);
- network of 5 GPS for automatic continuous measurements;
- 1 Total station measuring a total of 31 optical targets.

4 of the 31 optical targets, measured at an hourly rate, are positioned out of the rock slide limits on

stable ground by a total station positioned on the opposite valley side at the same station point adopted for the LisaLab GB-InSAR and the GPS reference station. The GB-InSAR equipment, installed since the beginning of the monitoring programme, allows for the displacement field monitoring (line of sight, LOS, displacement) every 9 minutes in cells of size ranging between 0.5 and 4.4 m at a distance between 500 m and 2000 m, respectively. The radar is positioned in a way so that the maximum slope displacement is roughly aligned with the LOS. 15 streaming points are monitored providing a continuous time history of their displacements. These displacement field maps have been used for a revision of geomorphological observations.
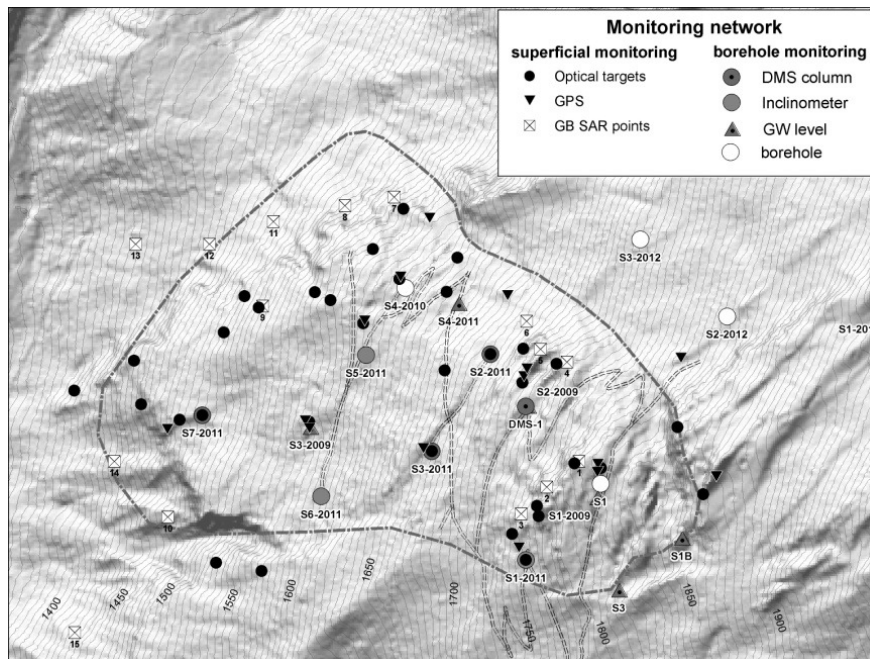
Figure 5. Position of the main elements forming the topographic and the geotechnical monitoring networks. GB-InSAR points show the position of the streaming points with continuous acquisition. DMS: multi-parametric probe; inclinometers: boreholes equipped with inclinometric casing; GW level: piezometers.

The GPS network is based on a set of single frequency stations which transmit phase data every 15 sec to the main controlling unit.

The geotechnical monitoring network includes:

- 6 Inclinometer casings for periodic measurements
- 3 borehole wire extensometers
- 6 Piezometers
- 4 DMS multi-parametric probes

and have been regularly updated because of the damages related to the large displacements causing failure of the inclinometric casing and open case piezometers. The 4 DMS columns range in length between 12 m and 110 m. In particular, one DMS column is 12 m long (monitoring between 58 and 80 of depth), 2 are 80 m long and one is 110 m long.

5.1 Data analysis

The availability of such a monitoring network generates a huge amount of data. In the following we try to present some of the data to demonstrate their reliability and the redundancy, as well the consistency between different measuring systems. EDM measurements (Figure 6a) provide a dataset for the initial phases of the study. They are useful but cannot be used to clarify the seasonal behavior of the rock slide and some of the data are of low quality because of the very simple approach used for the preparation of the station and measured points.
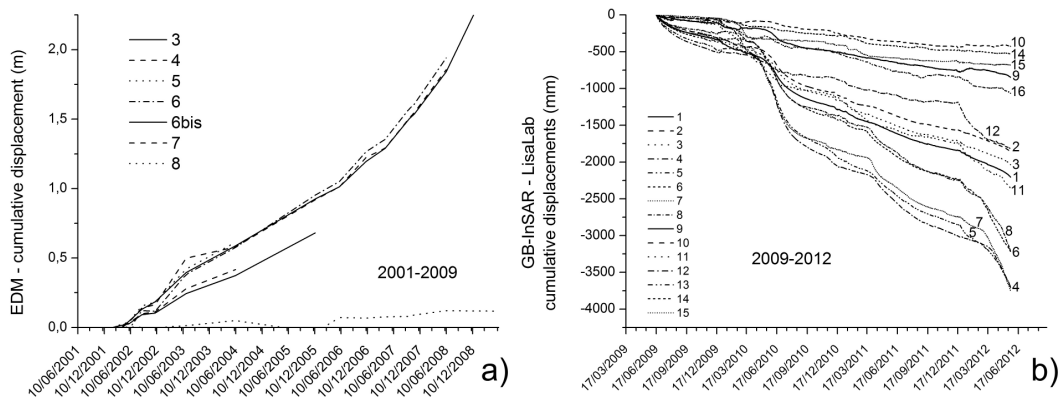
Figure 6. Cumulative displacements measured a) by EDM on optical targets between 2002-2009, and b) by the GB-InSAR LisaLab equipment between 2009 and 2012 for 15 streaming points (see Figure 4 for their location). Partial superposition of the measures by GPS, GB-InSAR and total station allowed for the attachment of the historical data series.

A much more precise and consistent dataset is the one related to the total station measurements (since June 2009) with soundly founded benchmarks and station points. The dataset shows a clear seasonal pattern with accelerations during the snow melting season (see Figure 7 for the 2010 season, Figure 8 for the entire monitoring period with GPS data, Figure 9 for a comparison between optical targets and GBR streaming points), with maximum cumulative displacements of about 5 m, and maximum seasonal displacements of about 2 m. In particular, Figure 7 shows the progressive acceleration with snow melting accompanied by the groundwater level increase, and the almost total independence on the rainfall input.

GB-InSAR data show a similar pattern in time and space and allow for the delineation of the most active slope sectors by the spatially distributed cover. Figure 10 shows some displacement maps generated by the LisaLab system and it puts into evidence the seasonal behavior to which the landslide is subjected. In particular, some important aspects of the slope movement are evidenced in a temporal sequence: the start of the displacements in early spring within the scree deposit at the landslide toe before the rock slide area; the rapid acceleration in the right hand sector of the landslide; the acceleration of the rock slide head sector; the restrained displacement of the toe debris during the acceleration of the rock slide; the relatively rapid deceleration of the movement in late summer.

Lacking other information up to now, this suggests a failure surface day-lighting at the base of the landslide rocky toe or at the apex of the scree deposit.
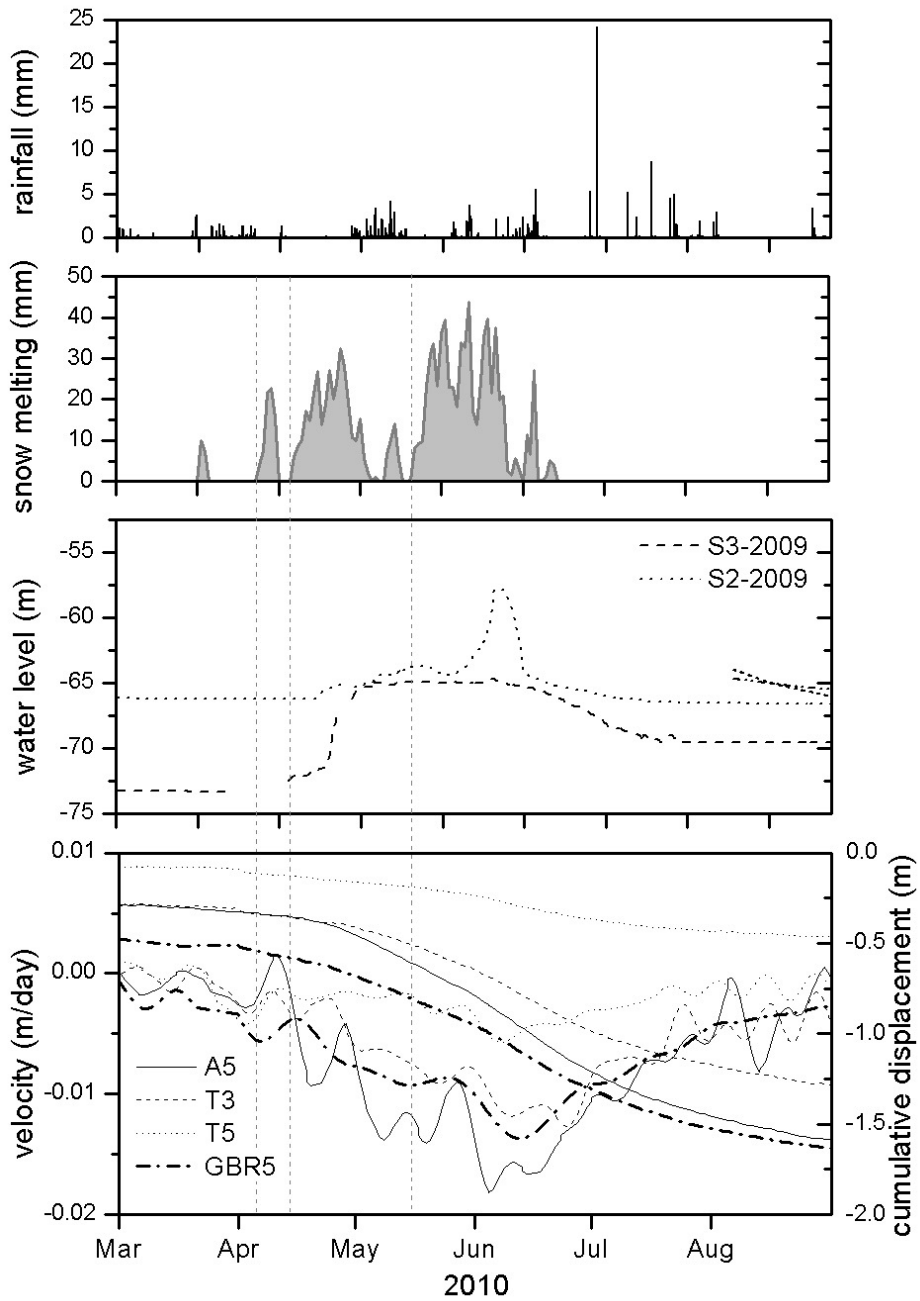
Figure 7. Comparison of target (A5, T3, T5) and GB-InSAR (GBR5) streaming point velocities and cumulative displacements with rainfall, snow melting and piezometric level during the 2009-2010 season. Hatched vertical lines points to the beginning of each major snow melting period.
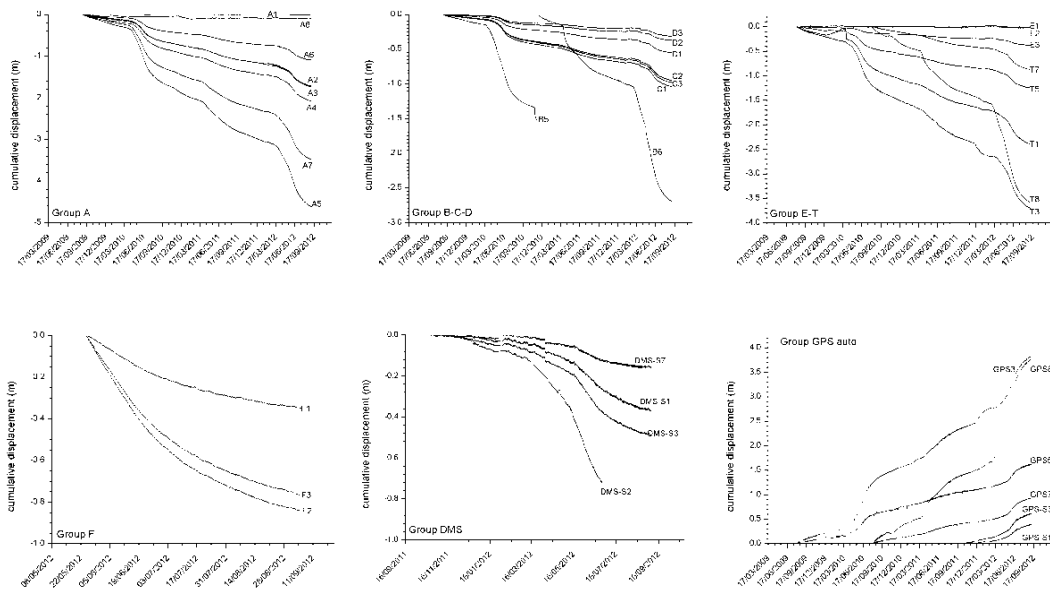
Figure 8- Cumulative displacement vs time for optical targets and the GPS automatic network. Optical targets are grouped according to different areas of the landslide.
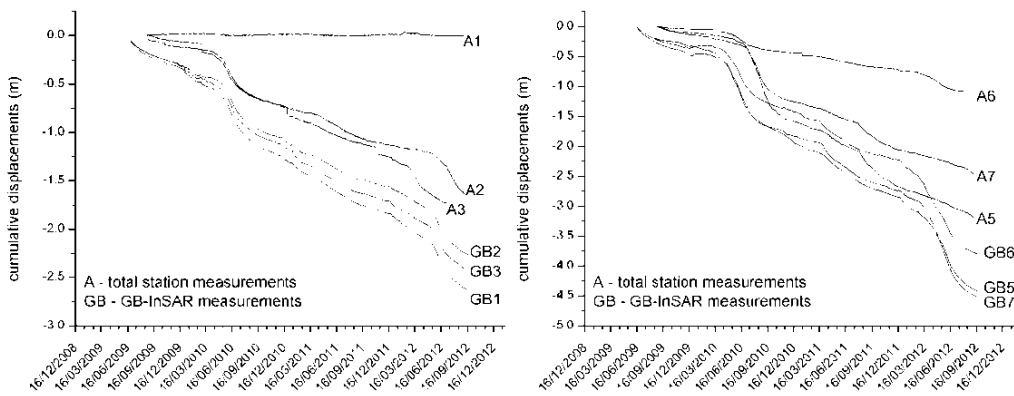

Figure 9. GB-InSAR streaming points (see Figure 5 for location) vs total station (optical targets) measurements for the same broad sectors of the rock slide. A1 is reported as reference point outside of the rockslide main scarp. A slight difference in the onset of the measuring of the two instruments cause the shift but the general pattern and total displacements are well comparable
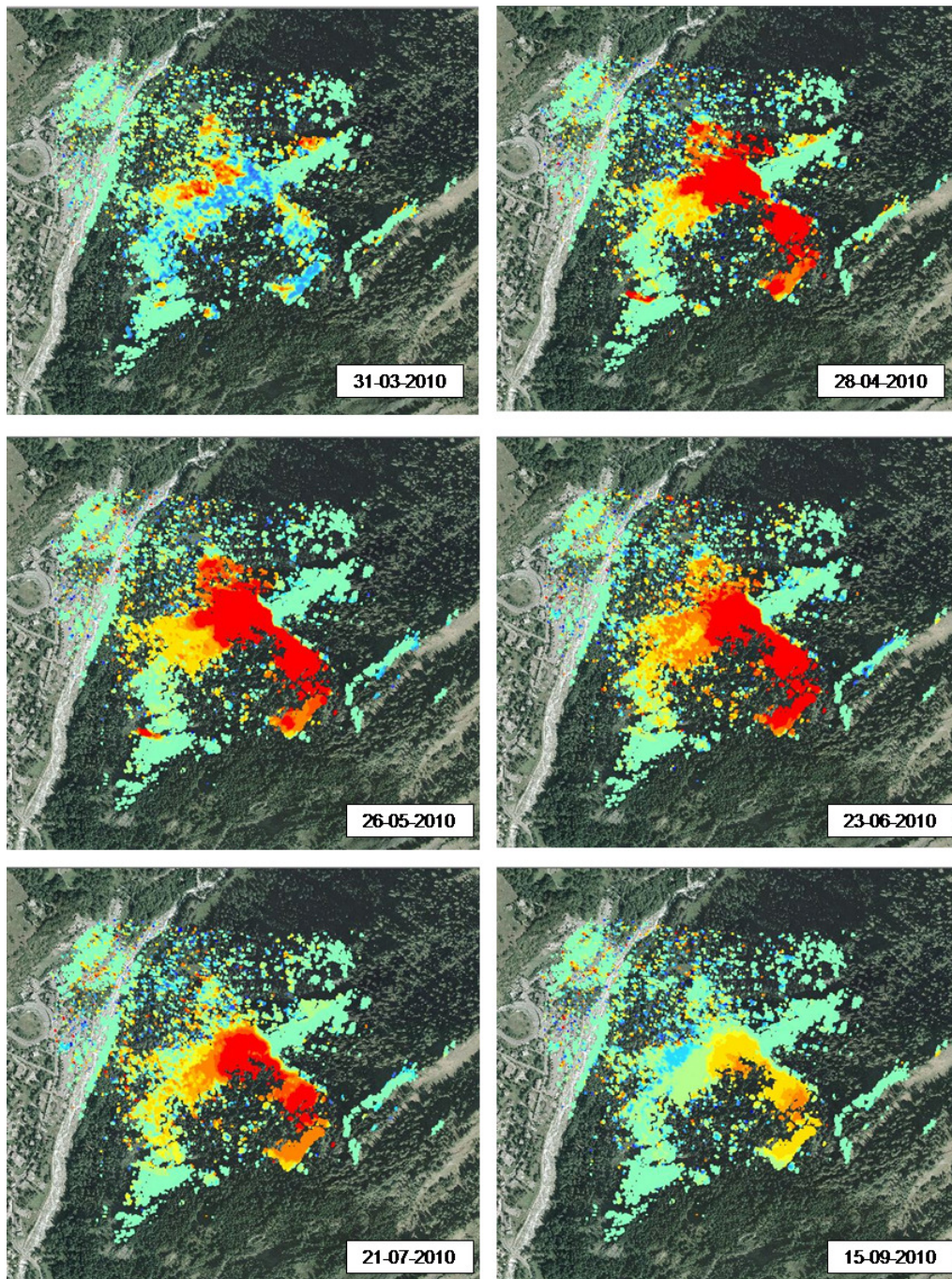
Figure 10. Monthly displacements maps, generated by the GB-InSAR LisaLab equipment in 2010, from early spring to late summer. These maps show the pattern of displacements and the sequential activation of sectors with different characteristics.

The quality of the measurements and the redundancy of the system is demonstrated by the agreement between measurements taken by means of different equipment (see Figure 6, 7, 8, 9 and 10).

Availability of inclinometric and multi parametric probes allow also for a comparison between superficial and deep movements and to verify the sensitivity of deep displacements to rainfall and snow melting. Figure 11 support the clear relationship between superficial and deep displacements. Superficial displacements start earlier and grow more progressively with respect to deep seated ones with an average delay of 7 to 10 days.
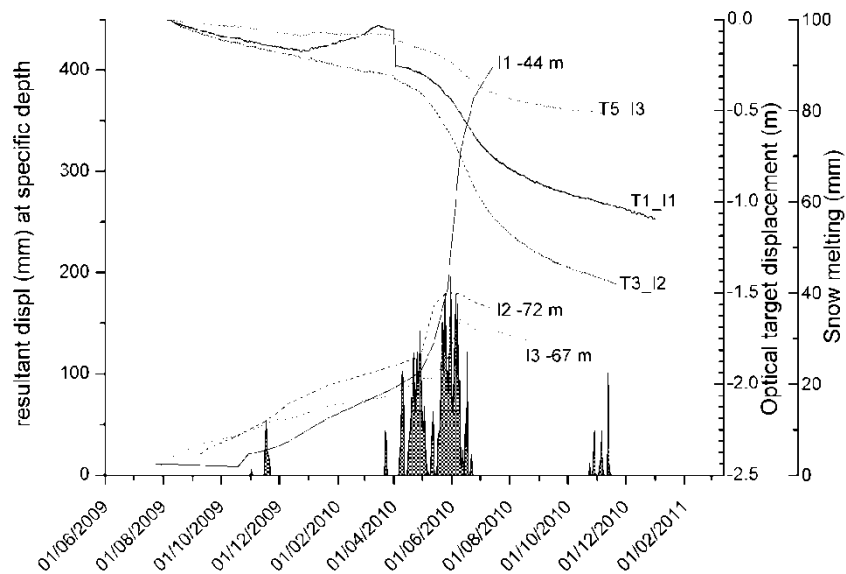
Figure 11. Plot of the total displacement measured by successive inclinometric measurements along the shear zone at three different sites(I1, I2, I3 and depths) and by total station measurements at points closest to the boreholes (T5_I3, T1_I1, T3_I2). Continuous constant slow movements during the winter time and rapid acceleration during snow melting (grey area) are visible in both the datasets.

6 Geometrical reconstruction

Borehole, inclinometric and DMS probes data allowed the reconstruction of the failure surface and of the limit between fractured and unfractured rock mass. By georeferencing and interpolation of the failure suface, along which most of the displacement occurs, it has been possible to compute the rock slide volume. Furthermore, the reconstructed failure surface has been compared to the direction of the superficial (see Figure 12) and deep displacements (inclinometer azimuth), observing that most of the displacement occurs in the direction of the maximum dip angle of the failure surface.

The resulting surface is an important outcome of the analysis because the failure geometry can influence the future evolution of the landslide mass and also the possible final collapse and spreading. Anyway, it must be stressed that the deep displacements occur sometimes above (20 to 40 m) the contact between intensely fractured and sound rock bedrock.

Piezometric data, collected through the years, allowed also to reconstruct the piezometric surface and its changes with time. We consider the piezometric surface as a minimum piezometric surface (also during the wet snow melting season) because of the use of open case piezometers. In fact this type of monitoring tools generally resist larger displacements but cannot give high resolution

and precise data (e.g. short-circuiting). In those cases where deep movements occur well above the limit between bedrock and fractured mass, the groundwater level lies well below the failure surface. This especially true for the upper boreholes located in proximity of the slide head.
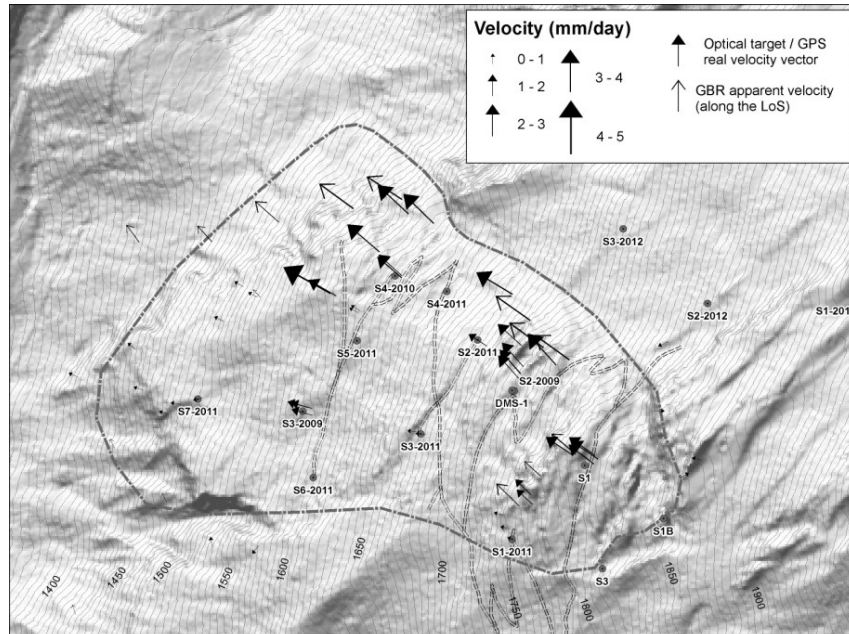

Figure 12. Map showing the average day velocity vectors measured along the unstable slope by the topographic network (total station and GPS) and by the GB-InSAR (along the LOS). For a comparison with more spatially distributed data see Figure 8 and Figure 4 for GB-InSAR streaming points.

7   Scenarios

The available data (GB-InSAR, optical targets, instability events) for the rockslide suggest that the failure plane probably daylights above the valley bottom and in proximity of the lower part of the toe rocky cliff. This condition suggests the possibility of a rapid collapse involving the entire rock slide mass (about $8 * 10^6$ m³), generating a fast moving rock avalanche which can spread along the valley bottom. The consequences could be catastrophic, affecting the Entrèves village, the state road and the highway, as well the access to the Mont Blanc highway and cableway. Therefore, a series of quasi 3D runout simulations have been run to define the invasion area and the deposit depth distribution. Definition of the invasion area permits the assessment of the level of expected damages, the identification of safe areas and routes for civil protection actions, the geometry of a possible impounded lake which could cause breaching or overtopping of the landslide dam.

This is clearly a major risk scenario but it can be complemented by a series of secondary or minor scenarios including small and intermediate flows and rock falls. As examples of such secondary risks, we mention the two rock falls (June 2008, May 2012), involving some hundred cubic meters of rock, detached from the toe rocky cliff. The blocks fell about 100 m reaching and crossing the Dora di Ferret river course endangering the large parking lot on the opposite side by projections of small rock fragments.

Because of the higher relative probability of occurrence of such minor scenarios and the potential impacts on urban areas, modeling of the phenomena and hazard zonation are requested by the

local administration.

8 Modeling

The different types of scenario require a series of different modeling approaches to be adopted for their analysis especially to cover all the possible consequences or secondary phenomena, as well for the relative uncertainties.

8.1 Landslide runout

Mathematical modeling of long runout landslides is still a debated research subject which requires some modeling skills, the knowledge of landslide behavior and the choice of the most suitable and possible scenarios. One of the problems in the case of the La Saxe rockslide, as well as for many other case studies, is the lack of antecedent events that could help at assigning realistic rheologic models and material properties to the landslide material. In these cases, the possible approach consists in adopting models and property values already tested and validated for many other case studies occurred under similar geological and environmental constrains. We used a 2.5 or quasi 3D (depth averaged) model in which the unstable mass volume was introduced (Chen and Lee, 2000; Chen et al, 2006; Crosta et al, 2004).

Results of the simulations are shown, as an example, in Figure 13 where the selected landslide geometry (limits and depth) is reported together with the deposit thickness distribution along the valley bottom. This deposit distribution is one of the input data for the dam breaching simulations. These required the definition of the river discharge, the average thickness of the deposit and of the erodible material, the extent of impounded water, the type of dam failure mechanism.
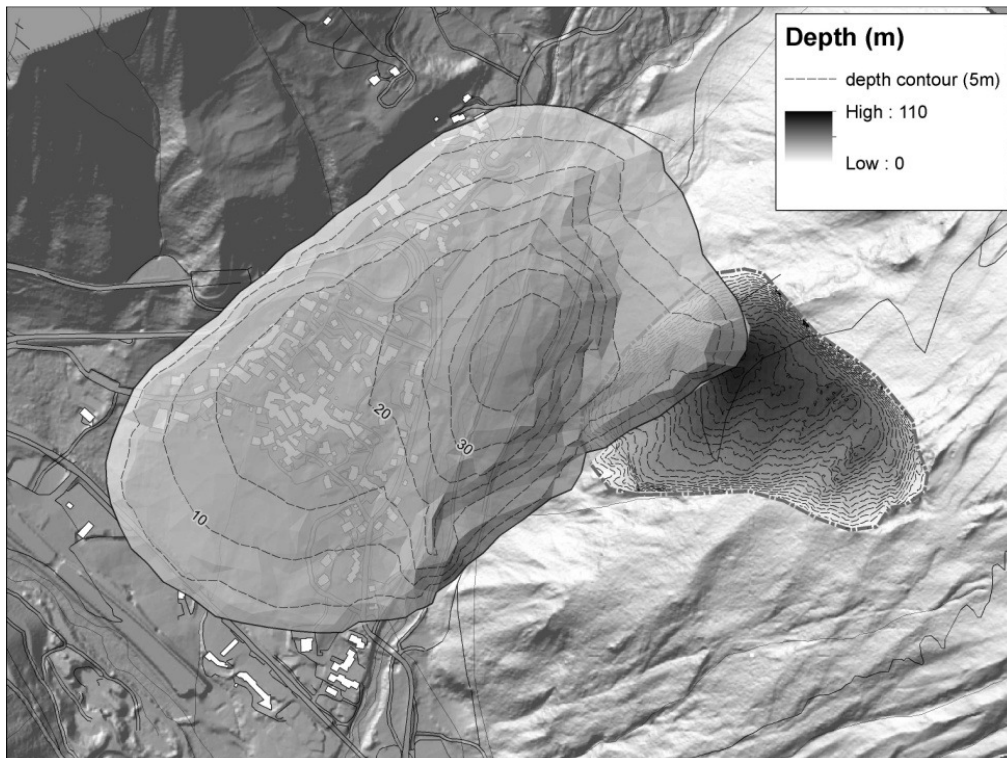

Figure 13. Result for a possible spreading of a $8 * 10^6$ m^3 rock avalanche scenario

8.2 Rockfalls

A similar approach has been followed to produce rock fall hazard zonation maps for minor failure scenarios. The simulations have been carried out by means of a 3D code (Hy-Stone, Crosta et al., 2004, Frattini et al, 2008, Agliardi et al, 2009). In this case two past events were available (2008 and 2012) and it was possible to perform some model calibration. The simulations allowed to set the limits of the most hazardous areas and to define the extent to which civil protection actions should be conducted.

8.3 Groundwater flow modeling

Hydrological and hydrogeological data have been used to accomplish an initial 2D and 3D groundwater flow modeling. The 3D models has been developed considering the strong rock anisotropy, the presence of a deep seated flow system and the possible recharge action played by a set of morpho-structures acting as runoff concentrators. These models showed that the contribution of concentrated infiltration can help at raising the groundwater level within the rock slide mass in a way similar to what observed during high seasonal discharges. These recharge episodes are quite rapid and controlled by the extremely high permeability of the trench material. This is shown by the model which also represents the consequent rapid rise of the deep regional groundwater table.

8.4 Slope stability analysis

For what concerns the slope stability assessment two series of preliminary analyses have been carried out according to the following aims:

- a preliminary evaluation of the effects related to the seasonal fluctuation of the piezometric surface on the global safety factor of the rockslide;

- a preliminary validation of the numerical 3D analyses with different constitutive models by reproducing the distribution of the monitored displacements.

These analyses didn't include the long term geologic evolution of the slope (e.g. deglaciation), but they are aimed only to the analyses of the present day conditions. As a consequence, they should then be considered as the preliminary step for a consistent 3D numerical modelling of the initiation phase of the rock-slide. Presently, more attention is dedicated to reproduce exhaustively the complex 3D geometry and boundaries. The involved materials have been described using perfect elasto-plastic constitutive models without any time dependent behaviour.

8.4.1 Influence of the piezometric fluctuation on the slope stability

As aforementioned, the slope displacements show a clear seasonal pattern with significant accelerations during the snow melting season suggesting that a fluctuation of the groundwater level of 8 m on average occurs within the slide. In Figure 14 a 3D synthesis of the geometrical and piezometric data is shown. Borehole and inclinometer data imposed the 3D failure surface geometry and the volume of the unstable mass (see Figure 14a), whereas the piezometric surface for the summer (maximun level, Fig. 14b) and winter season (minimum level) give the two limit conditions to be analysed.
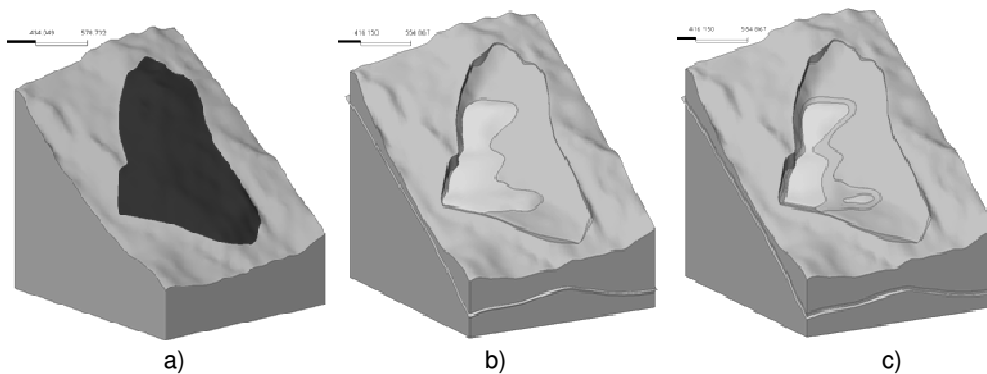
Figure 14. 3D solids: a) unstable mass in black; b) summer and c) winter GW levels in light grey.

A FEM mesh has been created splitting the rockslide in three regions (see Figure 15a) characterized by different geomechanical parameters defined on the basis of geomechanical field classifications, as well in situ and laboratory tests. A series of SSR (Shear Strength Reduction) static analyses were performed by considering the two extreme conditions. In Figure 15 the contours of displacement and plastic strain at failure are shown, while in Table 1 the adopted parameters at the different stages of the c-phi reduction analyses are summarized. In term of safety factor variation, the results shown an increment of approximately 15% when the piezometric level is lowered from the summer level to the winter one. This suggest that a possible mitigation measure to be considered is the creation of a proper drainage system to maintain the piezometric surface as lower as possible.
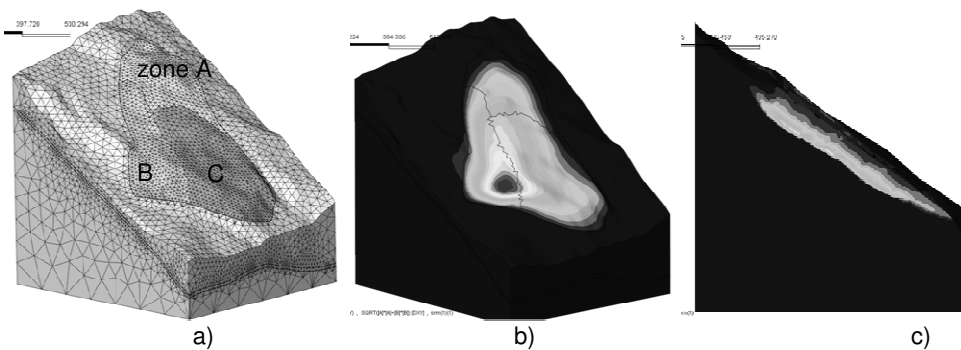

Figure 15: a) adopted mesh colored according to the subdivision in sectors of different properties; b) total displacement distribution at failure; c) equivalent plastic strain along a cross section.

Table 1. adopted parameters and safety factor variation under the two limit seasonal conditions.
SRF: Strength Reduction Factor

| | | γ [kN/m^3] | ϕ [°] | Cohesion [kPa] | | | SRF |
				Zone A	Zone B	Zone C	
Initial parameters		24	27	120	1	105	1
Parameters at failure	Summer GW level	24	13.76	58	2.08	50	2.08
	Winter GW level	24	11.94	50	2.41	44	2.41

8.4.2 Comparison with recorded displacements

This series of analyses is motivated by the need for the evaluation of the capability of the numerical model to reproduce the real failure surface and the spatial distribution of the superficial displacement. Consequently, in order to reproduce the rock-slide, only the lateral vertical constrains have been introduced with no limitation in depth for to the development of the failure surface. Two constitutive models based on perfect elasto-plasticity have been considered: i) the standard Mohr-Coulomb (MC) model with Hooke law for elastic behavior and Mohr-Coulomb criteria for yielding and failure, ii) the joint rock (JR) model that is an extension of MC-model allowing the failure to occur only along three predefined 3D discontinuity planes.

Additional constrains have been introduced by assigning different sets of geomechanical parameters at each one of the different zones (see Figure 16a and b) according to in situ evidences.

The results in term of prediction of failure surface are shown in Figure 16c and 16d for the MC model and JR model, respectively. By taking into account the main discontinuity sets it becomes evident the capability of the JR model to better reproduce the real failure surface as well as the spatial distribution of the normalized displacements (see Fig 16 e and f).

As further steps into numerical modeling, the time dependent behavior and viscous effects as well as large strains description will be introduced in order to reproduce the monitored displacement versus time trend and to provide reliable predictions.

9 EWS

One more step consisted in the use of the monitoring network for early warning purposes. This step has been iterated through the entire study to allow for: the setting up of preliminary alert threshold values for emergency action planning during the initial investigation phase; the verification of the temporary threshold values by comparison with observations collected during the monitoring; the definition or refining of the threshold values.

The initial thresholds (pre-alerting and alerting) were defined on previous experience on similar large rock slides (Crosta & Agliardi, 2002, 2003, Rose & Hungr, 2006) which underwent catastrophic collapses (1 mm/h and 2 mm/h, respectively). These values were compared continuously to the measured variables (displacement rate and acceleration) by the GPS, total station and LisaLab GB-InSAR data allowing for a redundant and spatially distributed analysis. Usually, with exception for some cases, the maximum observed displacement rate values have been ranging between 5 to 10 mm d^{-1}.

The overpassing of the threshold values is verified for each point and for multiple points contemporaneously, as well as for two or more successive overpassing by the same monitored point.

The validity of the preliminary threshold values has been proved by the May 2012 acceleration of a small sector of the slide toe, when the rock fall event was originated. In that case a timely alert has been sent out that allowed for the closure of the parking lot and the performing of some field surveys.

Finally, the availability of highly precise and accurate borehole instrumentation (DMS probes) allows the definition of thresholds also for deep seated displacements, occurring along the failure zone. DMS systems integrate an EWS management unit which can produce alarm calls when any of the modules passes the imposed threshold value.
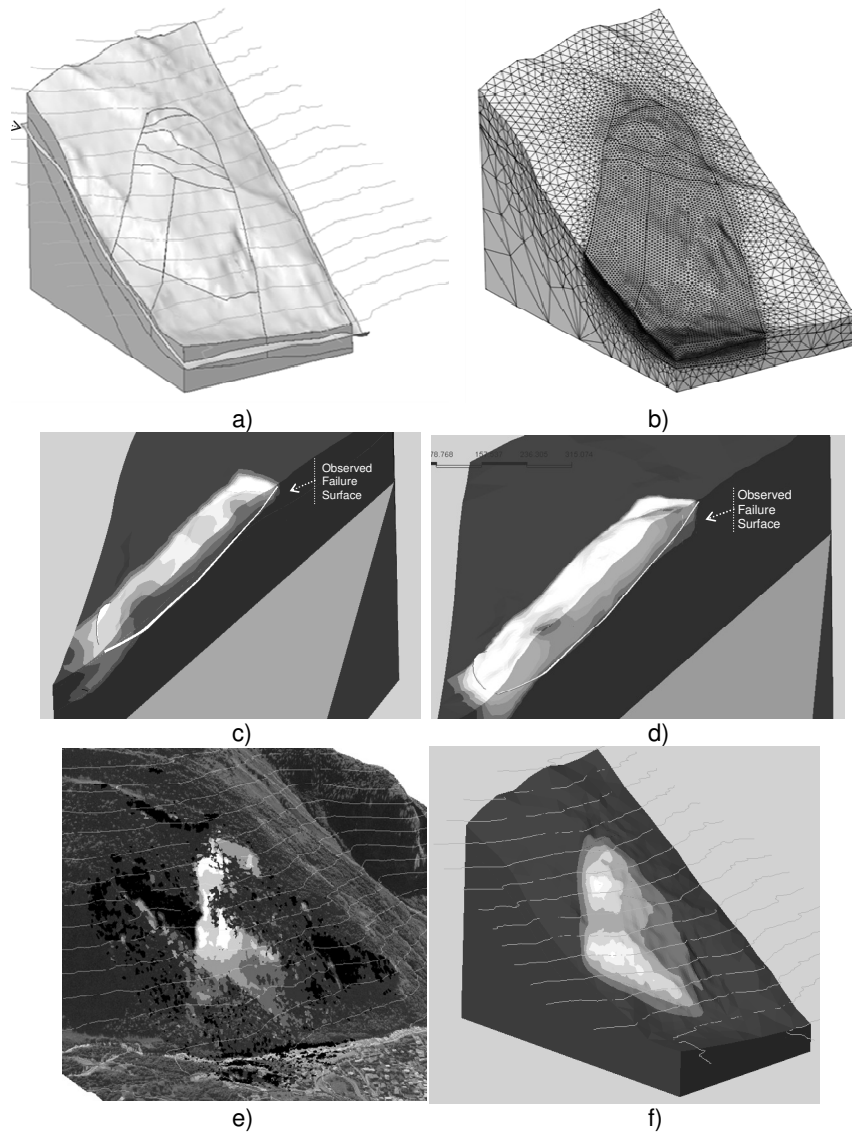
Figure 16: 3D solids: a) 3D geometrical model and internal zonation; b) 3D FEM mesh; c) plastic strain contours and failure surface predicted by MC model; d) plastic strain contours and failure surface predicted by JR model; e) normalized displacement as from GB-InSAR measurements; f) normalized displacement computed by adopting the JR model.

10 Conclusions

High risk phenomena characterized by complex settings require a careful description that is not always possible to accomplish. A case study of a rockslide under rapid evolution is reported and discussed, showing a possible approach to the definition of the main constraining factors and of the possible expected progress. The recognition of the more relevant factors and of the way they act at destabilizing the slope is not always an easy task and in rapid evolving phenomena this can be

extremely challenging. In fact, rapid evolution makes difficult the monitoring of repeated mechanisms controlling the failure.

11 Acknowledgements

12 References

Agliardi F., Crosta G.B., Frattini P. (2009) Integrating rockfall risk assessment and countermeasure design by 3D modelling techniques. Natural Hazards and Earth System Sciences, 9:1059-1073.

Chen, H. & Lee, C. F., 2000. Numerical simulation of debris flows. Can. Geotech. J., 37 (1), 146 -160.

Chen, H., Crosta, G. B. & Lee, C. F., 2006. Erosional effects on runout of fast landslides, debris flows and avalanches: a numerical investigation. Geotechnique, 56 (5), 305–322

Crosta GB, Agliardi F. Failure forecast for large rock slides by surface displacement measurements. Canadian Geotechnical Journal, 40; 1, 2003. 176–191.

Crosta, G., Agliardi, F., 2002. How to obtain alert velocity thresholds for large rockslides. Physics and Chemistry of the Earth 27 (2002), pp. 1557–1565.

Crosta, G. B., Chen, H. & Lee, C. F., 2004. Replay of the 1987 Val Pola Landslide, Italian Alps. Geomorphology, 60, 1–2, 127–146.

Crosta, G.B., Agliardi, F., Frattini, P. and Imposimato, S. (2004). A three-dimensional hybrid numerical model for rockfall simulation. Geophysical Research Abstracts, 6, 04502.

De Giusti F., Bonetto F., Dal Piaz G.V., 2005. Carta geologica della Valle d'Aosta, scala 1:100.000. Regione Autonoma Valle d'Aosta, Assessorato territorio, ambiente e opere pubbliche.

Frattini, P., Crosta, G.B., Carrara, A. and Agliardi, F. (2008). Assessment of rockfall susceptibility by integrating statistical and physically-based approaches. Geomorphology, 94, 419-437.

Ratto S., Giardino M., Giordan D., Alberto W., Armand M. 2007. Carta dei fenomeni franosi della Valle d'Aosta, scala 1:100.000. Regione Autonoma Valle d'Aosta, Assessorato Territorio, Ambiente e Opere Pubbliche, Tipografia Valdostana, Aosta.

Rose ND, Hungr O. Forecasting potential rock slope failure in open pit mines using the inverse-velocity method. Int J Rock Mech Min Sci 2006; 44:308–320.